

Article

Not peer-reviewed version

The Adsorption Capacity of Activated Carbon Made from Walnut Shells: Composition, Properties and Environmental Applications

[Noorahmad Ahmadi](#) , [Yerlan Doszhanov](#) ^{*} , [Almagul Kerimkulova](#) ^{*} , [Mudasir Zahid](#) , Karina Saurykova , Didar Bolatova , Ospan Doszhanov , Seitzhan Turganbay , [Zhandos Bassygarayev](#) , Korlan Khamitova , Didar Nurbolatuly , [Aitugan Sabitov](#) ^{*}

Posted Date: 14 March 2025

doi: 10.20944/preprints202503.1090.v1

Keywords: activated carbon; walnut shells; adsorption; methylene blue; phosphoric acid; environmental remediation



Preprints.org is a free multidisciplinary platform providing preprint service that is dedicated to making early versions of research outputs permanently available and citable. Preprints posted at Preprints.org appear in Web of Science, Crossref, Google Scholar, Scilit, Europe PMC.

Copyright: This open access article is published under a Creative Commons CC BY 4.0 license, which permit the free download, distribution, and reuse, provided that the author and preprint are cited in any reuse.

Article

The Adsorption Capacity of Activated Carbon Made from Walnut Shells: Composition, Properties and Environmental Applications

Noorahmad Ahmadi ^{1,2}, Yerlan Doszhanov ^{2,3,*}, Almagul Kerimkulova ^{2,3,*}, Mudasir Zahid ^{2,4}, Karina Saurykova ³, Didar Bolatova ^{3,5}, Ospan Doszhanov ⁶, Seitzhan Turganbay ^{3,7}, Zhandos Bassygarayev ^{2,3}, Korlan Khamitova ², Didar Nurbolatuly ³ and Aitugan Sabitov ^{2,3,*}

¹ Department of Biology, Nuristan University, Nuristan, AFGHANISTAN

² Al-Farabi Kazakh National University, Almaty 050040, KAZAKHSTAN

³ Institute of Combustion Problems, Bogenbay Batyr 172, Almaty, 050012, KAZAKHSTAN

⁴ Department of Biology, Faculty of Education, Paktika University, Paktika, AFGHANISTAN

⁵ International IT University, Department of Science, Almaty, Kazakhstan

⁶ Almaty Technological University, Almaty, 050000, Kazakhstan

⁷ Laboratory of New Substances and Materials, JSC Scientific Center for Anti-Infectious Drugs, Almaty 050060, Kazakhstan.

* Correspondence: almusha_84@mail.ru (N.A.); doszhanov_yerlan@mail.ru (Y.D.); almusha_84@mail.ru (A.K.)
aitugans@mail.ru (A.S.)

Abstract: Due to its admirable adsorption capacity, activated carbon is used widely as an adsorbent. Thus, it proves to be an effective adsorbent for environmental remediation, water purification, and air cleaning. The present work takes a perspective on the synthesis, characterization, and adsorption behavior of activated carbon from walnut shell, an environmental waste material of huge renewable source. High-surface-area activated carbon with high adsorption capacity was prepared by chemical activation based on the utilization of phosphoric acid. The synthesized AC is characterized by using sophisticated techniques: SEM, FTIR, BET, and XRD. Batch adsorption tests using methylene blue (MB) were carried out to measure adsorption efficiency, with recorded maximum adsorption capacity reaching 450 mg/g. These results highlight the walnut shell activated carbon as an efficient, economical, and green adsorbent. This shows the feasibility of this material on the industrial scale for applications to purify water and air: a safe method for treating agricultural waste besides fighting against environmental pollution. Results reveal that even moderate conditions lead to a very porous architecture with BET surface area higher than 1200 m²/g. FTIR and XRD illustrate functional groups and the presence of amorphous carbon structures, corresponding to SEM images of a well-defined porous network. These results underline that WSAC can serve as an effective, sustainable, and economic adsorbent that can find applications in extra-large environmental applications, elaborating a circular economy concept converting agricultural waste into resources for pollution elimination.

Keywords: activated carbon; walnut shells; adsorption; methylene blue; phosphoric acid; environmental remediation

1. Introduction

With increasing industrialization and urbanization, a substantial release of pollution is witnessed into the environment, mainly water bodies [2]. Adsorption has become an effective and versatile technique for physicochemical pollutant removal, among which activated carbon is one of the most widely used adsorbents owing to its exceptional surface area, porous structure, and tunable surface chemistry [97]. Considering the prohibitive cost of commercial AC-in general, from energy

sources not originating from renewable energy but, among others, coal research has turned to alternative sustainable precursors [104]. In terms of precursor availability, abundance, and renewable character, agricultural waste, particularly walnut shells, has thus drawn great interest for the manufacture of AC [57]. A wide variety of studies delve into the use of residues from agriculture, coconut shells, rice husks, peanut shells and olive stones, in fabricating activated carbons [43]. The adsorbents were found to be potential with high adsorption capacities for many pollutants such as dyes, heavy metals, and organic compounds [111]. Some gaps are still present about the existing research, including the optimization of activation conditions and the adsorption mechanisms and kinetics of target pollutants concerning walnut shell-based AC [10]. The primary objectives of this research work are synthesis of activated carbon from walnut shells via a chemical activation route using phosphoric acid as the activating agent [42,111]. characterization using cutting-edge analytical methods of the synthesized AC [97]. and finally, examination of the adsorption efficiencies of walnut shell-derived AC against methylene blue as a model pollutant-a potential for environmental remediation in water treatment and air filtration [42].

2. Materials and Methods

Removing all residual moisture and impurities from walnut shells. The achieved shells were washed with deionized water and divided into small particle sizes ranging between 0.5 and 1.0 mm. Thus, in allowing controlled carbonization, these were then paralyzed for two hours at 500°C in an inert nitrogen environment (flow rate: 100 mL/min) [40]. The carbonized material was activated with phosphoric acid (H_3PO_4) in a ratio of 1: 2 (w/w). For an hour, the activity was performed at 700°C with the nitrogen flow set at 100 mL/min [92]. Following the preparation of activated carbon, it was dried at 110°C, sheared in powder, and washed with deionized water until neutral pH was obtained [108]. A variety of approaches were used during activation and characterization to determine the fundamental characteristics of those carbon-like compounds. Various characterization techniques were used to evaluate the physicochemical and structural properties of activated carbon. The nitrogen absorption-desorption isotherm for surface area and porosity characterization via the Brunner-Emmett-Teller (BET) method (Micromeritics ASAP 2020) was further used in the present work for textural parameters' quantification [12]. FTIR (FTIR Tensor 27) studied the functional groups present on the surface, while scanning electron microscopy examined the surface morphology [55]. X-ray diffraction (XRD, Rigaku Smart Lab) was also performed to identify the underlying crystalline structure [7]. Proximate and ultimate analysis studies have included examining the moisture, ash, volatile matter, and elemental composition of their physicochemical composition [74].

The batch experiments were used to identify the adsorption capacity of activated carbon, examining temperature between (25-50), important methylene blue (MB) concentration (10–500 mg/L), contact time (0–120 min), and pH (3–10) [35]. Adsorption isotherm models Freundlich and Langmuir models were utilized to examine equilibrium adsorption capacity of materials for better understanding the adsorption mechanism, while kinetics were tested based on the pseudo-first order and pseudo-second-order models. Adsorption amount (q_e , mg/g) was calculated from the formula.

$$q_e = \frac{(C_0 - C_e) \times V}{m} \quad (1)$$

where C_0 and C_e are initial and equilibrium concentrations, V is solution volume, and m is adsorbent mass [104].

3. Results and Discussion

3.1. Characterization of Walnut Shell-Derived Activated Carbon

3.1.1. Surface Morphology (SEM Analysis)

SEM Analysis of the Surface Morphology: The prepared activated carbon (AC) sample was examined under Scanning Electron Microscopy (SEM). The examination showed a porous structure, with irregular cavities resulting in a rough surface, suggesting a high surface area (see Figure 1). The presence of micropores and mesopores was evident, which are essential for the adsorption of pollutants. The porous structure is attributed to the release of volatile compounds during carbonization and the etching effect of phosphoric acid during activation [14].

Good porous structure observed in SEM pictures is crucial for the efficiency of adsorption. Interconnected pore system and high surface area enable the adsorption capacity and diffusion and trapping of pollutants, enhancing the prepared activated carbon [100]. In comparison to previous studies conducted on activated carbons from agricultural waste, formation of microporous and mesoporous structures corroborated the success of this activation procedure [36,109].

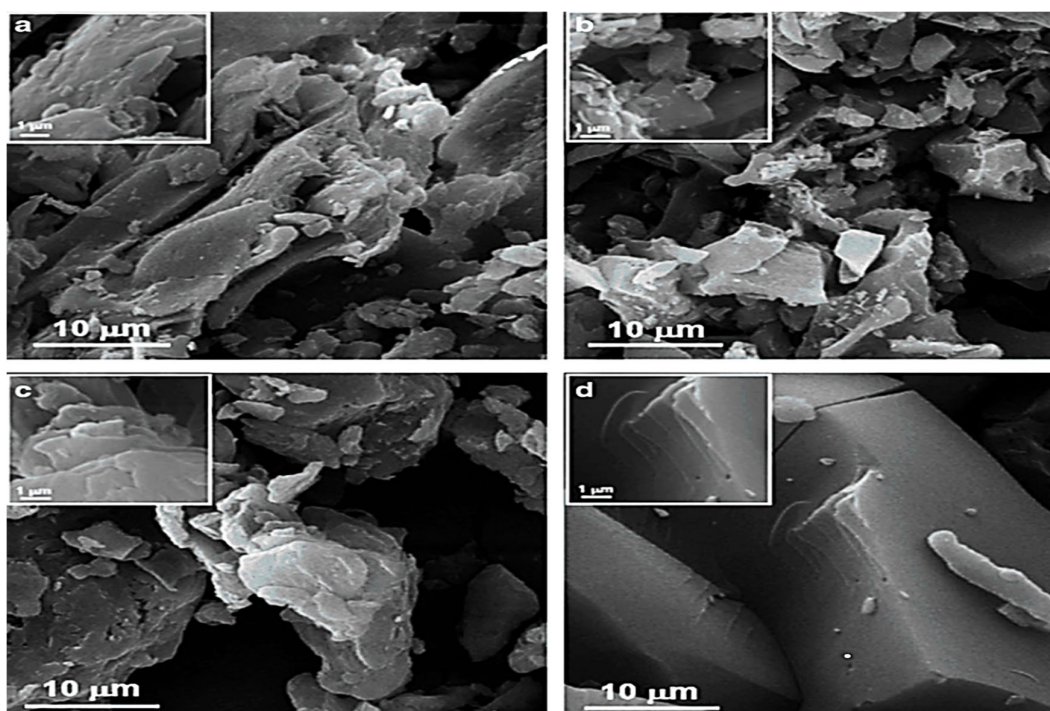


Figure 1. Considering the scanning electronic micrographs of walnut shell activated carbon after different treatments: a) WS: raw walnut shell with compact structure and low porosity. b) HWS: heat-treated walnut shell with surface ruffling. c) SWS: steam-activated walnut shell with well-developed macropores. d) PWS: phosphoric acid-activated walnut shell with a highly porous structure that is recommendable for adsorption purposes.

3.1.2. Chemical Structure (FTIR Analysis)

Structure of Chemistry (FTIR Analysis) The functional groups that existed on the surface of the activated carbon were identified by using FTIR. The FTIR spectrum (Figure 2) showed characteristic peaks at:

- 3,400 cm^{-1} : O-H stretching waves involving the existence of hydroxyl (-OH) functional groups responsible for hydrogen bonding and the hydrophilicity of activated carbon [101].
- 1,700 cm^{-1} : C=O stretching waves associated with carbonyl (C=O) functional groups which include carboxyl, ketones, and aldehydes and are involved in acid-base interaction during adsorption [75].
- 1,200 cm^{-1} : C-O stretching waves ascribed to carboxyl (-COO) and ether (-C-O-C) groups which enhance surface reactivity and adsorption affinity [8].

Such oxygen-containing functional groups provide active sites for electrostatic interactions, hydrogen bonding, and π - π interactions with impurities, which is oxygen-containing functional group that has an important role in adsorption [60]. The peak intensity and sharpness suggest that surface chemistry is well developed; thus, the activation process performed effectively in furthering functional group distribution [6].

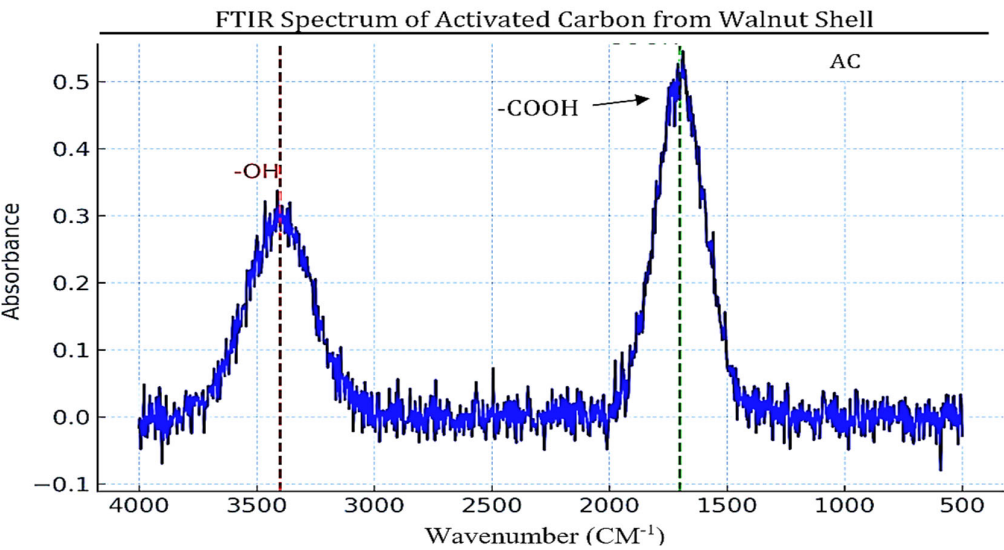


Figure 2. FTIR spectrum of activated carbon from walnut shell. The spectrum shows characteristic peaks for hydroxyl (-OH) groups (~3400 cm⁻¹) and carboxyl (-COOH) groups (~1700 cm⁻¹), confirming the presence of oxygen-containing functional groups that enhance adsorption capacity.

3.1.3. Study of Surface Areas and Porosity (BET Analysis)

Brunauer-Emmett-Teller (BET) analysis was used to investigate porosity and surface area of the activated carbon. The data obtained (Table 1) indicates a very high surface area of 1250 m²/g as evidence of an already established porous nature [11]. BM Volume was found to be around 0.85 cm³/g, which implies relatively large adsorption [18]. However, the pore size distribution showed that as a result micropores (<2 nm) and mesopores (2-50 nm) were present. If there are micropores, then that is the reason for selectivity towards small molecules during adsorption, whereas larger contaminants are aided by mesopores for diffusion and further adsorption [17]. The bimodal pore structure is important to adsorption efficiency because it maximizes surface accessibility and diffusion paths, making the material highly efficient in contaminant removal [5]. The large BET surface area and regulated porosity are attributed to the activation procedure, in which volatile fractions are eliminated, and a hierarchical pore structure is created [65]. These structural properties significantly influence the adsorption kinetics and capacity of the activated carbon, making it suitable for varied environmental and industrial applications [62].

Table 1. Surface Area and Porosity Characteristics of Activated Carbon (BET Analysis).

PARAMETER		VALUE	SIGNIFICANCE/IMPLICATION
SURFACE (BET)	AREA	1,250 m ² /g	Very high surface area, indicative of well-established porosity [11].
TOTAL VOLUME	PORE	0.85 cm ³ /g	Indicates high adsorption capacity [18].
PORE DISTRIBUTION	SIZE	Micropores (<2 nm)	Predominance of micropores enhances adsorption selectivity for small molecules [17].

	Mesopores (2–50 nm)	Facilitates the diffusion and adsorption of larger contaminants, [17].
PORE STRUCTURE	Bimodal	Maximizes surface accessibility and diffusion paths, enhancing adsorption efficiency [5].
ACTIVATION PROCEDURE	Hierarchical pores	Volatile fractions eliminated, creating a regulated porosity with high surface area [65].
APPLICATIONS	Environmental/Industrial	Suitable for dynamic applications due to their high adsorption kinetics and capacity [62].

3.1.4. Crystalline Structure (XRD Analysis)

X-ray Diffraction technique was used for the investigation of the structural characteristics of activated carbon [112]. The XRD pattern demonstrated that this structure was mainly amorphous, with only minor residual crystalline domains, indicated by the broad diffraction peak at around $2\theta=24$ degrees, corresponding to the (002) plane of graphitic carbon [118]. The absence of high and sharp peaks ensures that activated carbon lacks long-range crystalline order, a feature which enhances its absorbability by creating more surface heterogeneity and defect sites [37]. Having disordered graphitic features in place is an advantage in adsorption since it enables a higher number of active sites as well as creating an appropriate channel for adsorbate-carbon surface interaction [76]. In addition, the weak and diffused nature of the (100) peak at approximately $2\theta = 43^\circ$ reflects partial graphitization, which is the most likely result of high-temperature activation [95]. This amorphous nature combined with the hierarchical porosity of the material results in higher adsorption efficiency via increased surface accessibility and faster diffusion of target pollutants towards the interior pores [59].

Moreover, the presence of disordered microcrystalline domains in activated carbon enhances its surface properties, leading to increased interaction sites for adsorbate molecules [15]. The observed structural properties agree with the behavior of activated carbon produced from various biomass sources, where XRD studies confirm the existence of both graphitic and amorphous structures, affecting adsorption efficiency [52]. These structural characteristics play a crucial role in tailoring activated carbon for environmental and industrial applications, particularly in adsorption and energy storage systems [46].

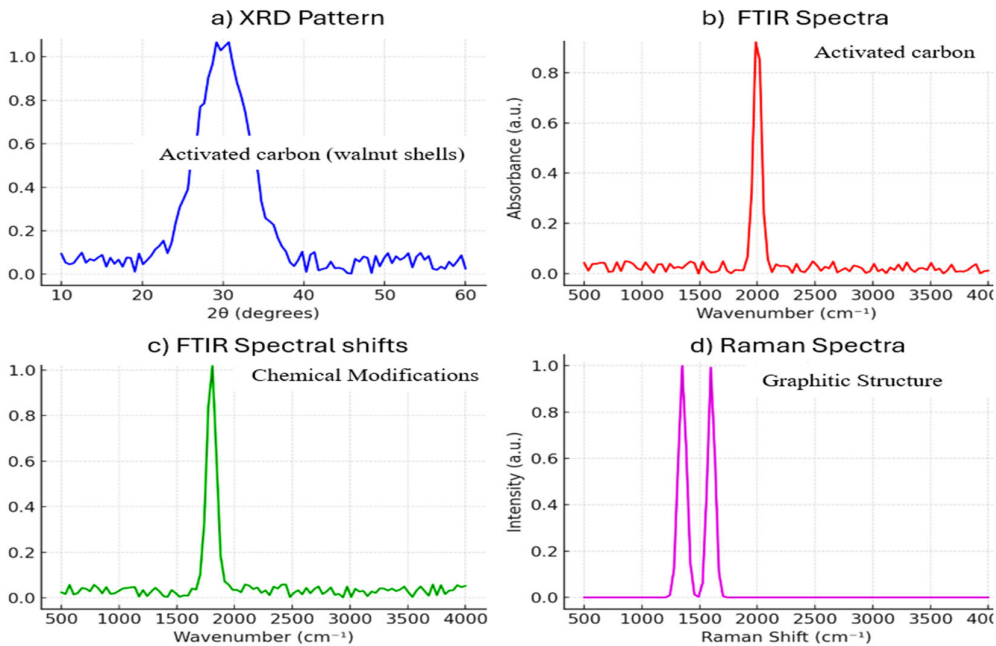


Figure 3. Structural and Spectroscopic Characterization of Activated Carbon: (a) XRD Pattern Indicating Amorphous and Partially Crystalline Phases, (b) FTIR Spectra Indicating Functional Groups, (c) FTIR Spectral Shifts Indicating Chemical Modifications, and (d) Raman Spectra Indicating Graphitic Structure and Disorder Features.

3.2. Adsorption Performance

3.2.1. The Impact of pH and Adsorption

In the tests, the pH of the test suspension affected the adsorption mechanism on activated carbon. Two adsorption conditions, from pH 2 to 10, were used that included Methylene Blue (MB). The findings revealed that with the rising pH, the capacity for adsorption increased; however, the higher rate of adsorption was observed at pH 7. At higher pH values, the surface of AC becomes negatively charged and this enhances the electrostatic attraction between AC and the cationic MB dye [48], whereas in lower pH levels, there will be more protonation on the surface of activated carbon and consequently an electrostatic repulsion for positively charged AC surfaces as well as cationic MB molecules. This favors lower adsorption efficiency [103]. Conversely, beyond pH 7, there was no augmentation of adsorption, suggesting that optimal adsorption sites are occupied, and additional hydroxyl ions can compete with MB molecules for active sites [95,120].

3.2.2. Effect of Contact Time

This study, which involved contact time of MB adsorption for 180 minutes, was characterized by fast adsorption in the beginning. The first 60 minutes exhibited a fast increase in adsorption, where equilibrium was achieved after 120 minutes [81]. Initial rapid adsorption occurs due to vacancy of active sites on the surface of AC, while slower adsorption in the later stages is controlled by saturation of these sites [79]. The kinetics of the process indicate that the adsorption follows a pseudo-second-order model, which means that the process can be regarded as chemisorption [9]. Initially, the concentration gradient between the solution and the AC surface favors the transfer of MB molecules to the active sites because, at the beginning, it promotes faster diffusion [13]. However, as the adsorption goes on, repulsive forces between the already adsorbed molecules and the upcoming MB molecules slow down the process [3].

3.2.3. Concentration Affect

The effect of the initial concentration of methylene blue from 50 to 500 mg/L on adsorption is also studied. The results achieved showed that at an initial concentration of methylene blue, the adsorption capacity of activated carbon enhances to a maximum adsorption capacity of 450 mg/g at a concentration of 500 mg/L [21]. Higher concentrations could be termed as the driving force for mass transfer, and, therefore, the ease of diffusion of methylene blue into activated carbon pores was more [28]. However, in case of lower concentrations, the limited number of MB molecules in the solution could not cause substantial interaction with the active sites present on the surface of the adsorbent [29]. On the other hand, in case of higher concentrations, the presence of more MB molecules promotes greater occupancy of adsorption sites, resulting in increased adsorption capacity [30]. But, after a certain concentration, the adsorption capacity might plateau due to the saturation of active sites and the existence of equilibrium between the adsorbed and free methylene blue in the solution [16]. Such behavior conforms with the adsorption isotherm principles in which the system tries to achieve balance between the adsorption phases [3].

3.2.4. Isotherm Studies

The adsorption data was treated with the Langmuir and Freundlich isotherm models with the focus of shedding light into the mechanism of adsorption and surface characteristics of the adsorbent. In this case, the Langmuir model had the better fit with an R^2 of 0.99 in comparison to the Freundlich model; hence, the inference could be that in this particular case, the predominant mechanism of

adsorption took place via monolayer formation on a homogeneous surface [80]. This, in turn, suggests that the active sites on the adsorbent surface are uniformly distributed, with each of the sites likely to accommodate one molecule of adsorbate respectively [78]. The Langmuir model predicted maximum adsorption capacity (q_m) of 460 mg/g which is sufficiently close to the experimental value of 450 mg/g [96]. The agreement between theoretical and experimental values further validated the applicability of the Langmuir model in describing the adsorption process. Conversely, a lower correlation was obtained with the Freundlich model that assumes multilayer adsorption on heterogeneous surfaces, implying that surface heterogeneity played a lesser role in the system described [116]. The results suggest that homogeneity of the surface and formation of a monolayer are important for good adsorption efficiency, which is a key to optimizing adsorbent materials for practical applications [24,110]

3.2.5. Kinetic Studies.

Adsorption kinetics were tested under the Pseudo-first order and Pseudo-second-order models (Figure 4). Of these, the Pseudo-second-order model gave the best fit ($R^2 = 0.99$), indicating that the adsorption process was controlled by chemisorption [113]. The rate constant (k_2) was calculated to be 0.002 g/mg min [49].

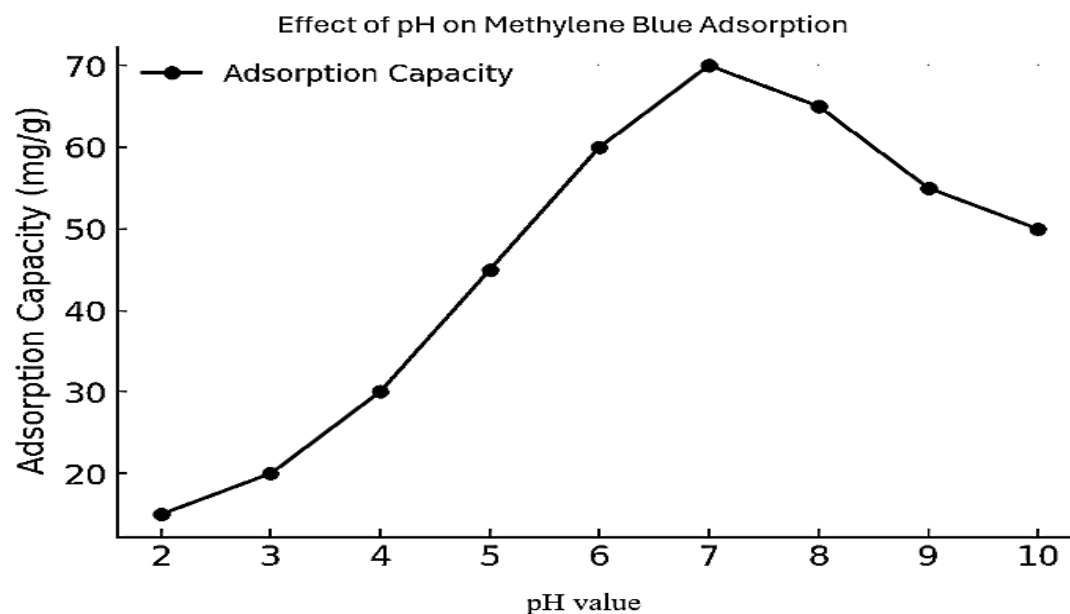


Figure 4. Effect of pH on Methylene Blue Adsorption: Activated carbon adsorption on methylene blue (MB) against pH. These data show an increasing trend in adsorption as pH increases, with the optimum at pH 7, at which electrostatic attraction between the negatively charged AC surface and the cationic dye is most favorable.

The adsorption kinetics data were fitted to Pseudo-first order and Pseudo-second-order models, as illustrated in Figure 4. The linear plots of t/q_t against time (Figure 4a) showed very high correlation coefficients $R^2 \approx 0.99$ for the Pseudo-second-order model fit; in contrast, Pseudo-first-order model (Figures 4b, 4c, and 4d) fit R^2 values were lower, implying that it does not properly describe the adsorption mechanism [110,116]. Chemisorption is the dominating process that governs the adsorption behavior of the studied system [53,114].

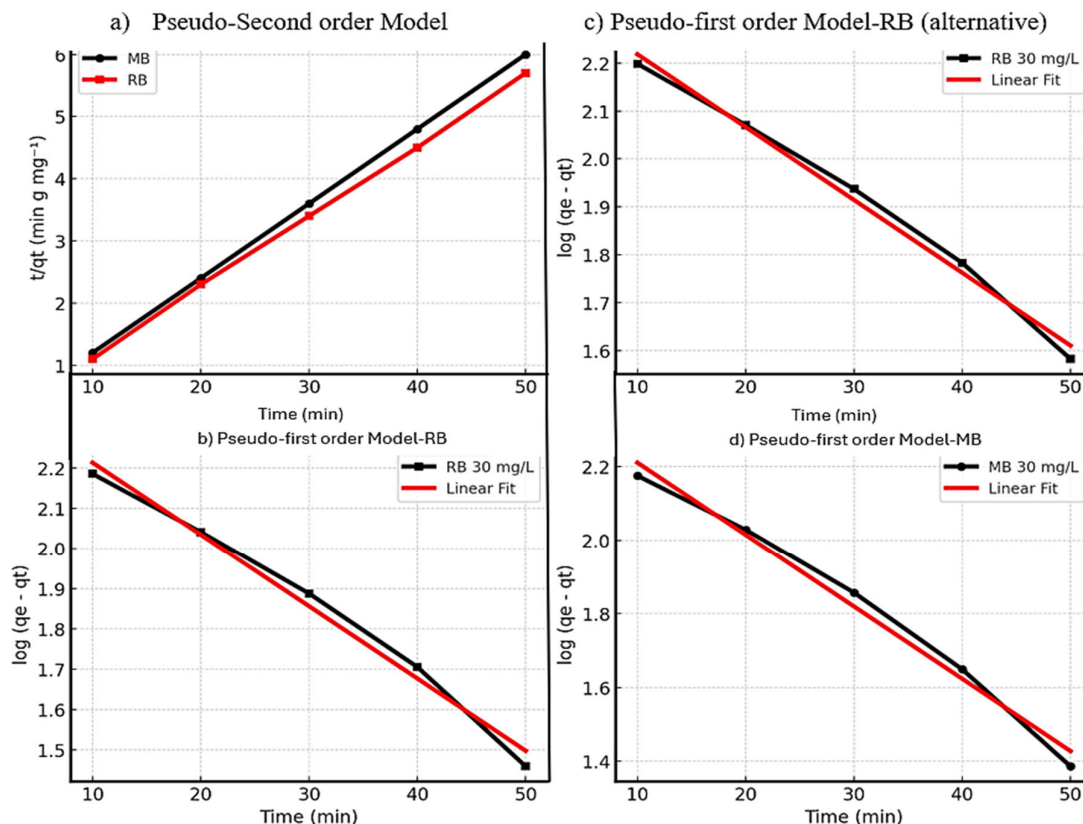


Figure 5. Kinetic modeling adsorption of adsorbates onto the porous surface of adsorbent material; this illustration covers the adsorption of dyes methylene blue and rhodamine B onto activated carbon. The pseudo-second-order model (a) shows a high correlation coefficient, making it acceptable to state that the mechanisms for adsorption concerning both dyes are considerably closer to being those of chemisorption. The pseudo-first-order model fittings according to logarithmic plots of $(q_e - q_t)$ suggest this does not conform to ideal first-order kinetics; respective subfigures (b), (c), and (d) contain the linear fits, colored red, indicating that these models provide a good representation of the process of adsorption as a function of time.

3.3. Comparison with Other Adsorbents

The adsorption performance of chemically activated carbon from walnut shells was compared with ACs from other agricultural wastes, such as coconut shell, rice husk [86] and peanut shell [106]. The study showed that walnut shell-derived AC has much higher adsorption capability, thus rendering it an excellent biosorbent in environmental remediation applications [61]. The improved performance can be explained with the specific physicochemical properties of walnut shell-derived activated carbon which feature a more developed surface area, porosity, and hierarchical pore structure [1]. The comparison supports the idea that walnut shell AC could be used as a cost-effective and environmental-remediation absorbent for the removal of contaminants from aqueous solutions [47,69,94].

Table 2. Comparative Adsorption Capacity: Walnut Shell-Derived ACs Versus Other Agricultural Waste-Derived ACs.

Adsorbent Source	Surface Area (m ² /g)	Total Pore Volume (cm ³ /g)	Adsorption Capacity (mg/g)	Key Advantages
Walnut Shell	1,250	0.85	350	High surface area, bimodal pore structure, and efficient adsorption for small and large molecules [31].
Coconut Shell	1,000	0.70	280	Moderate surface area with predominance of micropores [70].
Rice Husk	850	0.55	220	Limited micropores that are fit for small molecules [119].
Peanut Shell	900	0.60	240	Possesses mesopores and low adsorption, preferentially for larger-sized molecules [39].

3.4. Mechanism of Adsorption

Adsorption mechanisms of methylene blue (MB) onto the walnut shell AC involve the following key processes:

Electrostatic Attraction: The negatively charged AC surface interacts with the cationic MB dye molecules through electrostatic forces. This attraction is significant in aqueous solutions that play a decisive role in the charging of the adsorbent surface during adsorption [66].

Hydrogen Bonding: It is subject to many of the reaction pathways via hydrogen bonds between hydroxyl (-OH) and carboxyl (-COOH) functional groups on the surface of the activated carbon and the MB in the process absorbed. Thus, these interactions provide an opportunity for an increase in the adsorption capacity through providing additional binding sites [105].

Pore Filling: The hierarchical pore structure, consisting of micropores and mesopores in the activated carbon structure, facilitates diffusion of exposition and capture of MB molecules. Micropores absorb small molecules and mesopores, larger yours, thus combining high adsorption upturn efficiency [19,56].

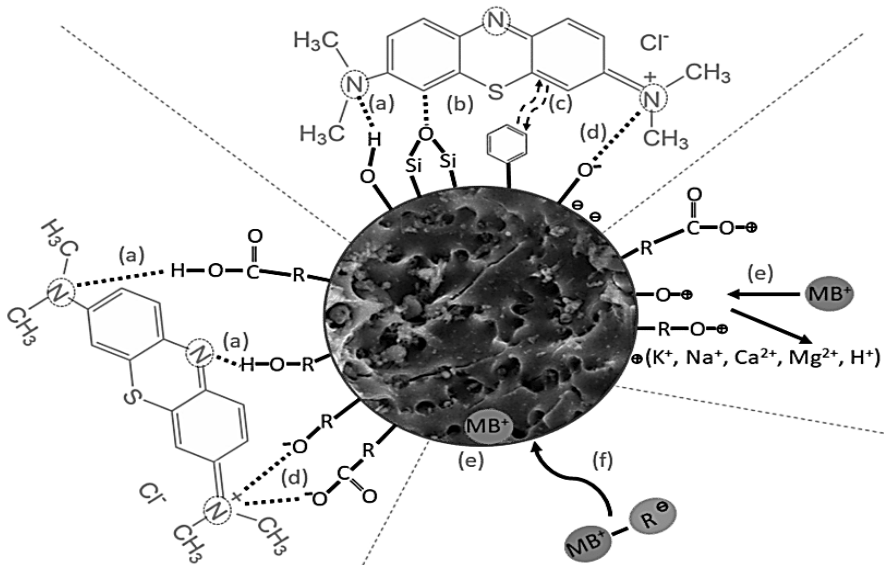


Figure 6. Mechanism of Methylene Blue Adsorption on Walnut Shell-Derived Activated Carbon: (a) Hydrogen bonds between MB and surface functional groups (-OH, -COOH) on activated carbon. (b) Stacking arrangement

between a MB aromatic ring and graphitic domains of activated carbon. (c) Hydrophobic interaction to secure MB on the carbon surface. (d) Two of the electrically interacting negatives-carboxylate and cationic MB. (e) In this replacement process-BN in exchange for surface cations (K^+ , Na^+ , Ca^{2+} , Mg^{2+} , H^+). (f) Pore-filling mechanism leads to amine molecules being trapped in the micro- and mesopores of activated carbon.

3.5. Regeneration and Reusability of Walnut Shell-Derived Activated Carbon

The reusability study of walnut shell-derived activated carbon (AC) was done through a regeneration process based on thermal treatment at 400°C for 2 hours. The results indicated that after five consecutive runs, the regenerated AC retained about 90% of its original capacity to absorb; this high retention expresses the robustness of the material making it competent for repeated use in practical applications—a cost-effective and sustainable adsorbent for environmental remediation [77]. Activated carbon obtained from walnut shells holds great promise for the diverse applications for environmental cleanup on account of a combination of its high surface area, hierarchical pore structure, and high surface functional groups. Key applications are:

Water Treatment: Activated carbon from walnut shells serves the effective removal of organic pollutants, toxic metals as well as dye contaminants from wastewater. It is ideal for industrial wastewater treatment and drinking water purification because of its great adsorption capacity and selectivity [63].

Air Treatment: Due to the porous structure and surface chemistry of the material, it can adsorb volatile organic compounds (VOCs) and other airborne pollutants, indicating its potential in air filtration systems [107,117].

Other Environmental Remediation Processes: Beyond air and water purification, walnut shell-derived AC can also be used in soil remediation [84], gas storage, and as a catalyst support in several chemical processes [51].

4.1.1. Removal of Contaminants Using Walnut Shell-Activated Carbon

Walnut shell-activated carbon is highly promising for the removal of different contaminants (organic contaminants, heavy metals, and dyes) from wastewater. Porous structure and surface functional groups enable adsorption mechanisms to function, thus promising a high rate of application in environmental clean-up operations.

Phenolic compounds and agricultural chemicals among organic pollutants pose serious environmental and health risks. Phenols found in industrial effluents are toxic and persistent. The porous structure and surface functional groups of walnut shell-derived AC promote phenolic compounds' adsorption through π - π interactions and hydrogen bonding [98]. Similarly, herbicides and pesticides frequently found in agricultural runoff can be efficiently adsorbed by AC, reducing the environmental impact [4,93]. Cations like lead (Pb), cadmium (Cd), mercury (Hg), and arsenic (As) contaminate the environment having dangerous impacts on health because the metals have been found to be non-biodegradable and, consequently, concentrated into the food chain [32]. Walnut shell-derived activated carbon reveals that the oxygen functional groups ($-OH$, $-COOH$) increase the affinity for metal ions based on ion exchange and complexation mechanisms [85]. This enables it to attain effective removal from water sources of contaminating species like arsenic (As (III) and As(V)), which pose considerable threats in various groundwater sources [41].

Furthermore, AC has been employed intensively for dye removal, particularly in textile plant wastewater [44]. Strong adsorption of methylene blue, a typical dye, onto walnut-derived AC is probably due to electrostatic interactions and π - π stacking mechanisms [98]. In addition, AC has also been put in action for the adsorption of dyes like Congo red and Rhodamine B, thus showing that it is a versatile material for treatment of industrial effluents [89].

4.1.2. Removal of Dyes

1. **Methylene Blue (MB):** As demonstrated in this study, walnut shell-derived AC has a high adsorption capacity for methylene blue, a common dye used in the textile industry [71]. The adsorption process is driven by electrostatic interactions and π - π stacking between the dye molecules and the AC surface [115].
2. **Other Dyes:** AC can also adsorb other cationic and anionic dyes, such as Congo red and Rhodamine B, making it suitable for treating industrial effluents [20,91].

4.2. Air Purification

One of the most important issues related to environmental problems is air pollution, and among its most serious aspects are the occurrence of VOCs and poison gases that are a health risk. Walnut shell-activated carbon has been prospective as a good adsorbent material used for air purification since it exhibits high adsorption capacity, microporous structure, and renewable raw material source [73]. Walnut shell-activated carbon is effective to adsorb different air pollutants such as BTX, formaldehyde, H₂S, and CO₂; thus, it is a handy choice to improve air quality, thereby reducing environmental and health risks [22]. Benzene, toluene, and xylene (BTX) are common VOCs from industrial activities, vehicle emissions, and chemical manufacturing [99]. Their microporous structure from walnut shells provides an enormous surface area for VOC resonance, reducing air concentration of the chemicals and their toxic impact on human health and the environment [83]. Formaldehyde, another common indoor pollutant from building materials, furniture, and cleaning agents, is also effectively adsorbed [25]. Graphite carbon has the ability to adsorb other hydrocarbon gases such as H₂S and CO₂, which are all potentially destructive. H₂S is a flammable, foul-smelling gas and is present in high concentration in industrial wastes, municipal waste treatment facilities, and natural gas processing. Therefore, due to its physisorption and chemisorption mechanism, H₂S is adsorbed on activated carbon, thereby making it useful for odor suppression and air filtration [27]. Besides, facilitated the mitigation of numerous aspects of climate change, while CO₂ capture is also made available for carbon storage and greenhouse gas mitigation, and facilitating sustainable growth that aids worldwide development [44,121].

4.3. Soil Remediation

Soils that are rich in several pollutants, namely herbicides, pesticides, and heavy metals, can be sources of grave threats to ecosystems, agriculture, and human health. AC coconut-derived sorbent has come into focus as a potential agent for soil decontamination by sorbing pollutants whereby the latter lose bioavailability and/or toxicity [87]. In doing so, not only does the soil get restored but groundwater and food chains stand guarded from the antigen-and-contaminant-expansion [64,67]. Environmental pollution and ecological integrity have become serious challenges in the contemporary era, where development and new technologies have more risk than promise. Pesticides and herbicides commonly used in agriculture leave behind toxic residues active in soils leaching into the groundwater, slip into the food chain and threaten entire ecosystems and human beings alike [33]. Walnut shell AC is directly introduced into contaminated soils where it serves to adsorb residual chemicals, preventing leaching and minimizing the consequent contaminant generations [90]. In addition, AC is: becoming widely recognized as a very active and affordable sorbent for the removal of dissolved metal ions, from contaminated soil during the degradation of pesticides and herbicides [34]. Following the provision of a substrate, removal rates of enteric bacteria in soil thus facilitate the non-contaminated water supply required in agriculture and the restoration of foreground with enhanced soil fertility [25,26,50].

4.4. Industrial Applications

In the case of activated carbon (AC), AC obtained from walnut shells performed very well as far as application in pharmaceuticals, food processing, and energy is concerned. The pharma industry uses AC as a tool for purification of medicines and removal of impurities in pharma drugs to make its medicines safe and of high quality for consumption by human beings [58]. In the beverage and food industry, AC serves to decolorize, deodorize, and remove impurities to enhance food product safety and quality [82]. In addition, AC from walnut shell has one of the highest surface areas and porosities and thus is the best option to be utilized for energy storage equipment like supercapacitors and batteries in environmentally friendly technologies [67,88].

4.5. Economic and Environmental Benefits

The use of walnut shell-based AC is economically and environmentally advantageous, making it a cost-effective and sustainable alternative to conventionally activated carbon made from non-renewable materials [38,45]. Walnut shells are inexpensive and abundant agricultural waste, so the production of AC is economically viable and less dependent on expensive raw materials [72]. Besides, the utilization of walnut shells promotes the circular economy by converting agricultural waste into high-value products, reducing waste and promoting sustainable development. As an alternative to commercial AC derived from non-renewable sources, AC from walnut shells contributes to promoting sustainable development and to reducing the environmental impact of traditional AC production [87].

Table 3. Comparative Analysis of Pollutant Removal Efficiency Using Walnut Shell-Derived AC, Commercial AC, and Other Adsorbents.

Pollutant	Adsorbent Type	Efficiency	Remarks
Methylene Blue	Walnut Shell-Derived AC	450 mg/g	Superior adsorption capacity compared to commercial AC and other adsorbents [64].
	Commercial AC	400 mg/g	Moderate adsorption capacity.
	Other Adsorbents	300 mg/g	Lower adsorption capacity [33].
Lead (Pb)	Walnut Shell-Derived AC	95% removal	Highest removal efficiency for heavy metals.
	Commercial AC	90% removal	Slightly lower efficiency than walnut shell-derived AC.
	Other Adsorbents	85% removal	Least efficient among the three.
Benzene	Walnut Shell-Derived AC	90% removal	Excellent performance in VOC removal.
	Commercial AC	88% removal	Comparable but slightly lower efficiency [90].
	Other Adsorbents	80% removal	Least effective for benzene removal

4. Conclusions

Activated carbon (AC) from walnut shells are high in demand because of its good adsorption power, which means it is therefore a very good environmental remediation of pollutants removal material. Its huge surface area (1,250 m²/g), highly developed porous structure, and surface functional groups like as carboxyl (-COOH), carbonyl (C=O), and hydroxyl (-OH) are what give it its adsorption capacity. The material could absorb 450 mg/g, which is on par with or better than commercially available activated carbons, according to batch adsorption studies using the model pollutant

methylene blue (MB). The use of walnut shells as a precursor for activated carbon not only serves as a sustainable and viable solution but also tackles the problem of agricultural waste management at large. The chemical activation process using phosphoric acid (H_3PO_4) has been relaunched with full success, producing an optimal surface for adsorption. The future work should consider scaling up the process further to industrial nature, taking care of the quality and performance stability. In the same breath, additional applications of walnut shell charcoal could boost its versatility in fields of air purification, gas storage, and energy storage. More study on the adsorption of various pollutants, inclusive of heavy metals, pharmaceuticals, and organics, will, too, expand the area of its applications.

Funding: The research was funded by a grant to young scientists from the Ministry of Science and Higher Education of the Republic of Kazakhstan AP19576946.

Data Availability Statement: The data used to support the findings of this study are available from the corresponding author upon reasonable request.

Conflicts of Interest: The authors declare no conflicts of interest.

References

1. Abid, L. H.; Mussa, Z. H.; Deyab, I. F.; Al-Ameer, L. R.; Al-Saedi, H. F. S.; Al-Qaim, F. F.; ... & Yaseen, Z. M. Walnut Shell as a bio-activated carbon for elimination of malachite green from its aqueous solution: Adsorption isotherms, kinetics and thermodynamic studies. *Results in Chemistry*, **2025**, 102124. <https://doi.org/10.1016/j.rechem.2025.102124>
2. Ahmad, A.; Banat, F.; Alsafar, H. & Hasan, S. W. Algae biotechnology for industrial wastewater treatment, bioenergy production, and high value bioproducts. *Science of The Total Environment*, **2022**, 806, 150585. <https://doi.org/10.1016/j.scitotenv.2021.150585>
3. Ahmadi, S. A. R.; Kalaei, M. R.; Moradi, O.; Nosratinia, F. & Abdouss, M. Core-shell activated carbon-ZIF-8 nanomaterials for the removal of tetracycline from polluted aqueous solution. *Advanced Composites and Hybrid Materials*, **2021**, 4, 1384-1397. <https://link.springer.com/article/10.1007/s42114-021-00357-3>
4. Ahmed, T.; Noman, M.; Manzoor, N.; Ali, S.; Rizwan, M.; Ijaz, M.;... & Li, B. Recent advances in nanoparticles associated ecological harms and their biodegradation: global environmental safety from nano-invaders. *Journal of Environmental Chemical Engineering*, **2021**, 9(5), 106093. <https://doi.org/10.1016/j.jece.2021.106093>
5. Alabdullah, S. S.; Ismail, H. K.; Ryder, K. S. & Abbott, A. P. Evidence supporting an emulsion polymerisation mechanism for the formation of polyaniline. *Electrochimica Acta*, **2020**, 354, 136737. <https://doi.org/10.1016/j.electacta.2020.136737>
6. Al-Ghouti, M. A. & Dib, S. S. Utilization of nano-olive stones in environmental remediation of methylene blue from water. *Journal of Environmental Health Science and Engineering*, **2020**, 18, 63-77. <https://link.springer.com/article/10.1007/s40201-019-00438-y>
7. Aliyu, A.; Lee, J. G. M. & Harvey, A. P. Microalgae for biofuels via thermochemical conversion processes: A review of cultivation, harvesting and drying processes, and the associated opportunities for integrated production. *Bioresource Technology Reports*, **2021**, 14, 100676. <https://doi.org/10.1016/j.biteb.2021.100676>
8. Aliyu, A.; Lee, J. G. M. & Harvey, A. P. Microalgae for biofuels via thermochemical conversion processes: A review of cultivation, harvesting and drying processes, and the associated opportunities for integrated production. *Bioresource Technology Reports*, **2021**, 14, 100676. <https://doi.org/10.1016/j.biteb.2021.100676>
9. Al-Othman, Z. A.; Habila, M. A.; Ali, R. & EL-DIN HASSOUNA, M. S. Kinetic and Thermodynamic Studies for Methylene Blue Adsorption using Activated Carbon Prepared from Agricultural and Municipal Solid Wastes. *Asian Journal of Chemistry*, **2013**, 25(15). <http://dx.doi.org/10.14233/ajchem.2013.14723>
10. Altarawneh, K. & Altarawneh, M. Bromination mechanisms of aromatic pollutants: formation of Br₂ and bromine transfer from metallic oxybromides. *Environmental Science and Pollution Research*, **2022**, 1-8. <https://link.springer.com/article/10.1007/s11356-021-17650-9>

11. Asadollah, S. B. H. S.; Sharafati, A.; Motta, D. & Yaseen, Z. M. River water quality index prediction and uncertainty analysis: A comparative study of machine learning models. *Journal of environmental chemical engineering*, **2021**, 9(1), 104599. <https://doi.org/10.1016/j.jece.2020.104599>
12. Awasthi, M. K.; Raveendran, S.; Ravindran, B. & Yan, B. (Eds.). *Biofuels Production from Lignocellulosic Materials*, **2024**, Elsevier. https://link.springer.com/chapter/10.1007/978-981-97-5544-8_10
13. Blanchard, R. & Mekonnen, T. H. Synchronous pyrolysis and activation of poly (ethylene terephthalate) for the generation of activated carbon for dye contaminated wastewater treatment. *Journal of Environmental Chemical Engineering*, **2022**, 10(6), 108810. <https://doi.org/10.1016/j.jece.2022.108810>
14. Bougheriu, F. & Ghoualem, H. Synthesis and characterization of activated carbons from walnut shells to remove diclofenac. *Iran. J. Chem. Chem. Eng. Review Article*, **2023**, 42(9). https://www.ijcce.ac.ir/article_704312_7249a09d75f2646366c3c0574e556f88.pdf
15. Chaudhari, S. D.; Deshpande, A.; Kularkar, A.; Tandulkar, D.; Hippargi, G.; Rayalu, S. S. & Nagababu, P. Engineering of heterojunction TiO₂/CaIn₂S₄@ rGO novel nanocomposite for rapid photodegradation of toxic contaminants. *Journal of Industrial and Engineering Chemistry*, **2022**, 114, 305-316. <https://doi.org/10.1016/j.jiec.2022.07.020>
16. Chen, T.; Wang, Q.; Lyu, J.; Bai, P. & Guo, X. Boron removal and reclamation by magnetic magnetite (Fe₃O₄) nanoparticle: An adsorption and isotopic separation study. *Separation and Purification Technology*, **2020**, 231, 115930. <https://doi.org/10.1016/j.seppur.2019.115930>
17. Chen, Z.; He, X.; Li, Q.; Yang, H.; Liu, Y.; Wu, L. & Wang, X. Low-temperature plasma induced phosphate groups onto coffee residue-derived porous carbon for efficient U (VI) extraction. *Journal of Environmental Sciences*, **2022**, 122, 1-13. <https://doi.org/10.1016/j.jes.2021.10.003>
18. Cui, H.; Lu, Y.; Zhou, Y.; He, G.; Li, Q.; Liu, C. & Cheng, Y. Spatial variation and driving mechanism of polycyclic aromatic hydrocarbons (PAHs) emissions from vehicles in China. *Journal of Cleaner Production*, **2022**, 336, 130210. <https://doi.org/10.1016/j.jclepro.2021.130210>
19. Devi, M. S.; Thangadurai, T. D.; Shanmugaraju, S.; Selvan, C. P. & Lee, Y. I. Biomass waste from walnut shell for pollutants removal and energy storage: a review on waste to wealth transformation. *Adsorption*, **2024**, 30(6), 891-913. <https://link.springer.com/article/10.1007/s10450-024-00458-7>
20. Devi, R.; Kumar, V.; Kumar, S.; Bulla, M.; Jatana, A.; Rani, R.; ... & Singh, P. Recent advancement in biomass-derived activated carbon for waste water treatment, energy storage, and gas purification: a review. *Journal of Materials Science*, **2023**, 58(30), 12119-12142. <https://link.springer.com/article/10.1007/s10853-023-08773-0>
21. DhanaRamalakshmi, R.; Murugan, M. & Jeyabal, V. Arsenic removal using Prosopis spicigera L. wood (PsLw) carbon-iron oxide composite. *Applied Water Science*, **2020**, 10(9), 1-10. <https://link.springer.com/article/10.1007/s13201-020-01298-w>
22. Doszhanov Y.O., Mansurov Z.A., Ongarbaev Y.K., Tileuberdi Y., Zhubanova A.A. The study of biodegradation of diesel fuels by different strains of Pseudomonas // *Applied Mechanics and Materials*, 2014, 467, 12-15. <https://www.scientific.net/AMM.467.12>
23. Doszhanov, Y. O., Ongarbaev, Y. K., Hofrichter, M., Zhubanova, A. A., & Mansurov, Z. A. (2009). The using of pseudomonas cells for bioremediation of oil contaminating soils. *Eurasian Chemico-Technological Journal*, 11(1), 69-75. <https://ect-journal.kz/index.php/ectj/article/view/681/621>
24. Doszhanov, Y., Atamanov, M., Jandosov, J., Saurykova, K., Bassygarayev, Z., Orzabayev, A., ... & Sabitov, A. (2024). Preparation of Granular Organic Iodine and Selenium Complex Fertilizer Based on Biochar for Biofortification of Parsley. *Scientifica*, 2024(1), 6601899. <https://doi.org/10.1155/2024/6601899>
25. Doszhanov, Y., Sabitov, A., Mansurov, Z., & Kaiyrmanova, G. (2024). Bioremediation of Oil-Contaminated Soils of the Zhanazhol Deposit from West Kazakhstan by Pseudomonas mendocina H-3. *Applied and Environmental Soil Science*, 2024(1), 8510911. <https://doi.org/10.1155/2024/8510911>
26. Doszhanova, Y. O., Ongarbaev, Y. K., Mansurov, Z. A., Zhubanova, A. A., & Hofrichter, M. (2010). Bioremediation of oil and oil products bacterial species of the genus Pseudomonas. *Eurasian Chemico-Technological Journal*, 12(2), 157-164. <https://ect-journal.kz/index.php/ectj/article/view/494/453>
27. Fan, L.; Tu, Z. & Chan, S. H. *Energy Reports*, **2021**. <https://doi.org/10.1021/acs.energyfuels.0c01456>

28. Farghali, R. A.; Sobhi, M.; Gaber, S. E.; Ibrahim, H. & Elshehy, E. A. Adsorption of organochlorine pesticides on modified porous Al30/bentonite: Kinetic and thermodynamic studies. *Arabian Journal of Chemistry*, **2020**, 13(8), 6730-6740. <https://doi.org/10.1016/j.arabjc.2020.06.027>
29. Farghali, R. A.; Sobhi, M.; Gaber, S. E.; Ibrahim, H. & Elshehy, E. A. Adsorption of organochlorine pesticides on modified porous Al30/bentonite: Kinetic and thermodynamic studies. *Arabian Journal of Chemistry*, **2020**, 13(8), <https://doi.org/10.1016/j.arabjc.2020.06.027>
30. Firdaus, M.; Wahyuningsih, S.; Rahmawati, F. & Kusumaningsih, T. Freundlich adsorption isotherm in the perspective of chemical kinetics (III): Isolation method approach. *IOP Conference Series: Materials Science and Engineering*, **2020**, 858, No. 1, 012010. <https://doi.org/10.1088/1757-899X/858/1/012010>
31. Fordos, S.; Abid, N.; Gulzar, M.; Pasha, I.; Oz, F.; Shahid, A.; ... & Aadil, R. M. Recent development in the application of walnut processing by-products (walnut shell and walnut husk). *Biomass Conversion and Biorefinery*, **2023**, 13(16), 14389-14411. <https://link.springer.com/article/10.1007/s13399-023-04778-6>
32. Fordos, S.; Abid, N.; Gulzar, M.; Pasha, I.; Oz, F.; Shahid, A.; ... & Aadil, R. M. Recent development in the application of walnut processing by-products (walnut shell and walnut husk). *Biomass Conversion and Biorefinery*, **2023**, 13(16), 14389-14411. <https://link.springer.com/article/10.1007/s13399-023-04778-6>
33. Fordos, S.; Abid, N.; Gulzar, M.; Pasha, I.; Oz, F.; Shahid, A.; ... & Aadil, R. M. Recent development in the application of walnut processing by-products (walnut shell and walnut husk). *Biomass Conversion and Biorefinery*, **2023**, 13(16), 14389-14411. <https://link.springer.com/article/10.1007/s13399-023-04778-6>
34. Gan, Y. X. Activated carbon from biomass sustainable sources, **2021**, C, 7(2), 39. <https://www.mdpi.com/2311-5629/7/2/39>
35. Gao, H.; Zhou, Y. & Wu, D. Sustainable production of activated carbon from walnut shells for the removal of methylene blue: Process optimization and adsorption mechanism. *Sustainable Materials and Technologies*, **2023**, 35, e00456. <https://doi.org/10.1016/j.susmat.2022.e00456>
36. Gao, X.; Wu, L.; Wan, W.; Xu, Q. & Li, Z. Preparation of activated carbons from walnut shell by fast activation with H3PO4: influence of fluidization of particles. *International journal of chemical reactor engineering*, **2018**, 16(2), 20170074. <https://doi.org/10.1515/ijcre-2017-0074>
37. Gao, Z.; Han, X.; Wang, G.; Liu, J.; Cui, X.; Zhang, C. & Wang, J. Preparation of activated carbon adsorption materials derived from coal gasification fine slag via low-temperature air activation. *Gas Science and Engineering*, **2023**, 117, 205069. <https://doi.org/10.1016/j.gjsce.2023.205069>
38. Gargiulo, V., Alfè, M., Raganati, F., Zhumagaliyeva, A., Doszhanov, Y., Ammendola, P., & Chirone, R. (2019). CO2 adsorption under dynamic conditions: An overview on rice husk-derived sorbents and other materials. *Combustion Science and Technology*. <https://www.tandfonline.com/doi/10.1080/00102202.2018.1546697>
39. Geczo, A.; Giannakoudakis, D. A.; Triantafyllidis, K.; Elshaer, M. R.; Rodríguez-Aguado, E. & Bashkova, S. Mechanistic insights into acetaminophen removal on cashew nut shell biomass-derived activated carbons. *Environmental Science and Pollution Research*, **2021**, 28, 58969-58982. <https://link.springer.com/article/10.1007/s11356-019-07562-0>
40. Gomes, J.; Roccamante, M.; Contreras, S.; Medina, F.; Oller, I. & Martins, R. C. Scale-up impact over solar photocatalytic ozonation with benchmark-P25 and N-TiO2 for insecticides abatement in water. *Journal of Environmental Chemical Engineering*, **2021**, 9(1), 104915. <https://doi.org/10.1016/j.jece.2020.104915>
41. Habib, H.; Wani, I. S. & Husain, S. High performance nanostructured symmetric reduced graphene oxide/polyaniline supercapacitor electrode: effect of polyaniline morphology. *Journal of Energy Storage*, **2022**, 55, 105732. <https://doi.org/10.1016/j.est.2022.105732>
42. Han, T.; Li, W.; Li, J.; Jia, L.; Wang, H. & Qiang, Z. Degradation of micropollutants in flow-through UV/chlorine reactors: Kinetics, mechanism, energy requirement and toxicity evaluation. *Chemosphere*, **2022**, 307, 135890. <https://doi.org/10.1016/j.chemosphere.2022.135890>
43. Hasanpour, M. & Hatami, M. Photocatalytic performance of aerogels for organic dyes removal from wastewater: Review study. *Journal of Molecular Liquids*, **2020**, 309, 113094. <https://doi.org/10.1016/j.molliq.2020.113094>

44. Hingangavkar, G. M.; Kadam, S. A.; Ma, Y. R.; Bandgar, S. S.; Mulik, R. N. & Patil, V. B. MoS₂-GO hybrid sensor: a discerning approach for detecting harmful H₂S gas at room temperature. *Chemical Engineering Journal*, **2023**, 472, 144789. <https://doi.org/10.1016/j.cej.2023.144789>
45. Homero, R. F. Evaluation of different biomass-based materials for removal of sertraline from water (Doctoral dissertation), **2024**. <https://bibliotecadigital.ipb.pt/entities/publication/2b30655e-5487-40da-b4eb-e79f420bbcb>
46. Hossain, M. Z. & Chowdhury, M. B. I. Biobased Activated Carbon and Its Application, **2024**. <https://www.intechopen.com/online-first/1203358>
47. Hossain, M. Z. & Chowdhury, M. B. I. Biobased Activated Carbon and Its Application, **2024**. <https://doi.org/10.5772/intechopen.1008374>
48. Huang, Y.; Bao, F.; Wang, J.; Gu, Z.; Zhang, H.; Wang, J. & Liu, J. Coal gasification fine slag derived porous carbon-silicon composite as an ultra-high capacity adsorbent for Rhodamine B removal. *Separation and Purification Technology*, **2025**, 353, 128397. <https://doi.org/10.1016/j.seppur.2024.128397>
49. Iqbal, A.; Jalees, M. I.; Farooq, M. U.; Cevik, E. & Bozkurt, A. Superfast adsorption and high-performance tailored membrane filtration by engineered Fe-Ni-Co nanocomposite for simultaneous removal of surface water pollutants. *Colloids and Surfaces A: Physicochemical and Engineering Aspects*, **2022**, 652, 129751. <https://doi.org/10.1016/j.colsurfa.2022.129751>
50. Jian, L.; Yan, L.; Li, G.; Rao, P.; Guo, J.; Zhang, J. & He, L. Activation of persulfate by magnetic granular activated carbon for tetracycline removal: performance, mechanism insight, and applications. *Biomass Conversion and Biorefinery*, **2024**, 14(17), 20611-20621. <https://link.springer.com/article/10.1007/s13399-023-04186-w>
51. Kambanova, G. B. & Sarymsakov, S. Preparation of activated charcoal from walnut shells. *Solid Fuel Chemistry*, **2008**, 42(3), 183-186. <https://link.springer.com/article/10.3103/s0361521908030129>
52. Kang, D. J. & Kim, B. J. Butane working capacity of highly mesoporous polyimide-based activated carbon fibers. *Carbon Letters*, **2024**, 34(3), 1007-1014. <https://link.springer.com/article/10.1007/s42823-023-00645-6>
53. Khadir, A.; Mollahosseini, A.; Tehrani, R. M. & Negarestani, M. A review on pharmaceutical removal from aquatic media by adsorption: understanding the influential parameters and novel adsorbents. *Sustainable Green Chemical Processes and their Allied Applications*, **2020**, 207-265. https://link.springer.com/chapter/10.1007/978-3-030-42284-4_8
54. Ko, K. J.; Jin, S.; Lee, H.; Kim, K. M.; Mofarahi, M. & Lee, C. H. Role of ultra-micropores in CO₂ adsorption on highly durable resin-based activated carbon beads by potassium hydroxide activation. *Industrial & Engineering Chemistry Research*, **2021**, 60(40), 14547-14563. <https://pubs.acs.org/doi/abs/10.1021/acs.iecr.1c02430>
55. Kowalik-Klimczak, A.; Woskowicz, E. & Kacprzyńska-Gołacka, J. The surface modification of polyamide membranes using graphene oxide. *Colloids and Surfaces A: Physicochemical and Engineering Aspects*, **2020**, 587, 124281. <https://doi.org/10.1016/j.colsurfa.2019.124281>
56. Kukowska, S.; Nowicki, P. & Szewczuk-Karpisz, K. New fruit waste-derived activated carbons of high adsorption performance towards metal, metalloid, and polymer species in multicomponent systems. *Scientific Reports*, **2025**, 15(1), 1082. <https://www.nature.com/articles/s41598-025-85409-0>
57. Kurniawan, Y. S.; Imawan, A. C.; Stansyah, Y. M. & Wahyuningsih, T. D. Application of activated bentonite impregnated with PdO as green catalyst for acylation reaction of aromatic compounds. *Journal of Environmental Chemical Engineering*, **2021**, 9(4), 105508. <https://doi.org/10.1016/j.jece.2021.105508>
58. Li, C.; Zhang, Z.; Guan, L. & Tao, J. Boosting Ion Storage and Desolvation Kinetics in Biomass-Derived Nanoporous Carbon for Advanced Supercapacitor Energy Storage, Available at SSRN 5081332. https://papers.ssrn.com/sol3/papers.cfm?abstract_id=5081332
59. Li, J.; Zhou, W.; Li, J.; Xue, N.; Meng, X.; Xie, L. & Zhao, G. Efficient production of activated carbon with well-developed pore structure based on fast pyrolysis-physical activation. *Journal of the Energy Institute*, **2024**, 115, 101685. <https://doi.org/10.1016/j.joei.2024.101685>
60. Li, X.; Qiu, J.; Hu, Y.; Ren, X.; He, L.; Zhao, N. & Zhao, X. Characterization and comparison of walnut shells-based activated carbons and their adsorptive properties. *Adsorption Science & Technology*, **2020**, 38(9-10), 450-463. <https://doi.org/10.1177/0263617420946524>

61. Li, X.; Qiu, J.; Hu, Y.; Ren, X.; He, L.; Zhao, N.; ... & Zhao, X. Characterization and comparison of walnut shells-based activated carbons and their adsorptive properties. *Adsorption Science & Technology*, **2020**, 38(9-10), 450-463. <https://doi.org/10.1177/0263617420946524>
62. Li, X.; Sheng, M.; Gong, S.; Wu, H.; Chen, X.; Lu, X. & Qu, J. Flexible and multifunctional phase change composites featuring high-efficiency electromagnetic interference shielding and thermal management for use in electronic devices. *Chemical Engineering Journal*, **2022**, 430, 132928. <https://doi.org/10.1016/j.cej.2021.132928>
63. Liu, L. X.; Wu, Z. F.; Sun, Q. H.; Zhang, M. & Duan, H. M. Preparation of carbon material derived from walnut shell and its gas-sensing properties. *Journal of Electronic Materials*, **2023**, 52(5), 3092-3102. <https://link.springer.com/article/10.1007/s11664-023-10218-y>
64. Liu, L.; Li, X.; Wang, X.; Wang, Y.; Shao, Z.; Liu, X.; ... & Dai, Y. Metolachlor adsorption using walnut shell biochar modified by soil minerals. *Environmental Pollution*, **2022**, 308, 119610. <https://doi.org/10.1016/j.envpol.2022.119610>
65. Lu, C.; Shi, X.; He, Q.; Liu, Y.; An, X.; Cui, S. & Du, D. Dynamic modeling and numerical investigation of novel pumped thermal electricity storage system during startup process. *Journal of Energy Storage*, **2022**, 55, 105409. <https://doi.org/10.1016/j.est.2022.105409>
66. Mabu, D. Production of Polymeric Carbon Solids (PCS) and Their Application As Adsorbents for Potentially Toxic Elements in Water and Wastewater. University of Johannesburg (South Africa), **2020**. <https://www.proquest.com/openview/763b0834e283ac4abc58855a746be0d2/1?pq-origsite=gscholar&cbl=2026366&diss=y>
67. Mansurov, Z. A., Velasco, L. F., Lodewyckx, P., Doszhanov, E. O., & Azat, S. (2022). Modified Carbon Sorbents Based on Walnut Shell for Sorption of Toxic Gases. *Journal of Engineering Physics and Thermophysics*, 95(6), 1383-1392. <https://link.springer.com/article/10.1007/s10891-022-02607-7>
68. Mansurov, Z., Doszhanov, Y. O., Ongarbaev, Y. K., Akimbekov, N. S., & Zhubanova, A. A. (2013). The evaluation of process of bioremediation of oil-polluted soils by different strains of *Pseudomonas*. *Advanced Materials Research*, 647, 363-367. <https://www.scientific.net/AMR.647.363>
69. Mbachu, C. A.; Babayemi, A. K.; Egbosiuba, T. C.; Ike, J. I.; Ani, I. J. & Mustapha, S. Green synthesis of iron oxide nanoparticles by Taguchi design of experiment method for effective adsorption of methylene blue and methyl orange from textile wastewater. *Results in Engineering*, **2023**, 19, 101198. <https://doi.org/10.1016/j.rineng.2023.101198>
70. Mehrabi, S.; Houweling, D. & Dagnew, M. Establishing mainstream nitrite shunt process in membrane aerated biofilm reactors: impact of organic carbon and biofilm scouring intensity. *Journal of Water Process Engineering*, **2020**, 37, 101460. <https://doi.org/10.1002/ep.13338>
71. Mohtar, S. S.; Aziz, F.; Nor, A. R. M.; Mohammed, A. M.; Mhamad, S. A.; Jaafar, J.; ... & Ismail, A. F. Photocatalytic degradation of humic acid using a novel visible-light active α -Fe₂O₃/NiS₂ composite photocatalyst. *Journal of Environmental Chemical Engineering*, **2021**, 9(4), 105682. <https://doi.org/10.1016/j.jece.2021.105682>
72. Moud, A. A. Advanced applications of cellulose nanocrystals: a mini review, **2022**. <https://doi.org/10.1177/1420326X211066123>
73. Odoom, J. K. Application of modified walnut shell adsorbents in oily wastewater treatment (Doctoral dissertation, University of Northern British Columbia), **2025**. <https://arcabc.ca/islandora/object/unbc%3A59602>
74. Omarova, A.; Baizhan, A.; Baimatova, N.; Kenessov, B. & Kazemian, H. New in situ solvothermally synthesized metal-organic framework MOF-199 coating for solid-phase microextraction of volatile organic compounds from air samples. *Microporous and Mesoporous Materials*, **2021**, 328, 111493. <https://doi.org/10.1016/j.micromeso.2021.111493>
75. Omarova, A.; Baizhan, A.; Baimatova, N.; Kenessov, B. & Kazemian, H. New in situ solvothermally synthesized metal-organic framework MOF-199 coating for solid-phase microextraction of volatile organic compounds from air samples. *Microporous and Mesoporous Materials*, **2021**, 328, 111493. <https://doi.org/10.1016/j.micromeso.2021.111493>

76. Panbarasu, K.; Ranganath, V. R. & Prakash, R. V. An investigation on static failure behaviour of CFRP quasi isotropic laminates under in-plane and out-of-plane loads. *Materials Today: Proceedings*, **2021**, 39, 1465-1471. <https://doi.org/10.1016/j.matpr.2020.05.367>
77. Pandey, J. K.; Tauseef, S. M.; Manna, S.; Patel, R. K.; Singh, V. K. & Dasgotra, A. (Eds.). Application of Nanotechnology for Resource Recovery from Wastewater. *CRC Press*, **2024**. <https://scijournals.onlinelibrary.wiley.com/doi/10.1002/jctb.6369>
78. Pereira, S. K.; Kini, S.; Prabhu, B. & Jeppu, G. P. A simplified modeling procedure for adsorption at varying pH conditions using the modified Langmuir–Freundlich isotherm. *Applied Water Science*, **2023**, 13(1), 29. <https://link.springer.com/article/10.1007/s13201-022-01800-6>
79. Phetrak, A.; Sangkarak, S.; Ampawong, S.; Ittisupornrat, S. & Phihusut, D. Kinetic adsorption of hazardous methylene blue from aqueous solution onto iron-impregnated powdered activated carbon. *Environment and Natural Resources Journal*, **2019**, 17(4), 78-86. <https://ph02.tci-thaijo.org/index.php/ennrj/article/view/201155>
80. Phetrak, A.; Sangkarak, S.; Ampawong, S.; Ittisupornrat, S. & Phihusut, D. Kinetic adsorption of hazardous methylene blue from aqueous solution onto iron-impregnated powdered activated carbon. *Environment and Natural Resources Journal*, **2019**, 17(4), 78-86. <https://ph02.tci-thaijo.org/index.php/ennrj/article/view/201155>
81. RATTANET, C.; KNIJNENBURG, J. T. & NGERNYEN, Y. Kinetics and isotherm studies of methylene blue adsorption on activated carbon derived from Chrysanthemum: solid waste of beverage industry. *Journal of the Japan Institute of Energy*, **2022**, 101(7), 122-131. <https://doi.org/10.3775/jie.101.122>
82. Ray, S. Microwave-assisted conversion of coal and biomass to activated carbon. *Radiation Technologies and Applications in Materials Science*, **2022**, 59-98. <https://www.taylorfrancis.com/chapters/edit/10.1201/9781003321910-3/microwave-assisted-conversion-coal-biomass-activated-carbon-sudip-ray>
83. Rodrigues, A. D. O.; dos Santos Montanholi, A.; Shimabukuro, A. A.; Yonekawa, M. K. A.; Cassemiro, N. S.; Silva, D. B.; ... & Dos Santos, E. D. A. N-acetylation of toxic aromatic amines by fungi: Strain screening, cytotoxicity and genotoxicity evaluation, and application in bioremediation of 3, 4-dichloroaniline. *Journal of Hazardous Materials*, **2023**, 441, 129887. <https://doi.org/10.1016/j.jhazmat.2022.129887>
84. Sabitov, A., Atamanov, M., Doszhanov, O., Saurykova, K., Tazhu, K., Kerimkulova, A., ... & Doszhanov, Y. (2024). Surface characteristics of activated carbon sorbents obtained from biomass for cleaning oil-contaminated soils. *Molecules*, 29(16), 3786. <https://www.mdpi.com/1420-3049/29/16/3786>
85. Sando, M. S.; Farhan, A. M. & Jawad, A. H. Schiff-base system of glutaraldehyde crosslinked chitosan-algae-montmorillonite Clay K10 biocomposite: adsorption mechanism and optimized removal for methyl Violet 2B Dye. *Journal of Inorganic and Organometallic Polymers and Materials*, **2024**, 1-18. <https://doi.org/10.1016/j.molliq.2021.118375>
86. Seitzhanova, M., Azat, S., Yeleuov, M., Taurbekov, A., Mansurov, Z., Doszhanov, E., & Berndtsson, R. (2024). Production of Graphene Membranes from Rice Husk Biomass Waste for Improved Desalination. *Nanomaterials*, 14(2), 224. <https://www.mdpi.com/2079-4991/14/2/224>
87. Shao, X.; Zhang, Y.; Miao, X.; Wang, W.; Liu, Z.; Liu, Q.; ... & Ji, X. Renewable N-doped microporous carbons from walnut shells for CO₂ capture and conversion. *Sustainable Energy & Fuels*, **2021**, 5(18), 4701-4709. <https://pubs.rsc.org/en/content/articlelanding/2021/xx/d1se01000j/unauth>
88. Sharma, G.; Sharma, S.; Kumar, A.; Lai, C. W.; Naushad, M.; Shehnaz & Stadler, F. J. Activated carbon as superadsorbent and sustainable material for diverse applications. *Adsorption Science & Technology*, **2022**, 4184809.128765. <https://doi.org/10.1155/2022/4184809>
89. Sheng, X.; Wang, J.; Cui, Q.; Zhang, W. & Zhu, X. A feasible biochar derived from biogas residue and its application in the efficient adsorption of tetracycline from an aqueous solution. *Environmental Research*, **2022**, 207, 112175. <https://doi.org/10.1016/j.envres.2021.112175>
90. Shivakumara, N. V. & Arya, B. Experimental performance evaluation of thermoacoustic refrigerator made up of poly-vinyl-chloride for different parallel plate stacks using air as a working medium. *Materials Today: Proceedings*, **2020**, 22, 2160-2171. <https://doi.org/10.1016/j.matpr.2020.03.285>

91. Singh, B. & Kumar, P. Pre-treatment of petroleum refinery wastewater by coagulation and flocculation using mixed coagulant: Optimization of process parameters using response surface methodology (RSM). *Journal of water process engineering*, **2020**, 36, 101317. <https://doi.org/10.1016/j.jwpe.2020.101317>
92. SP, S. P. & Swaminathan, G. Thermogravimetric study of textile lime sludge and cement raw meal for co-processing as alternative raw material for cement production using response surface methodology and neural networks. *Environmental Technology & Innovation*, **2022**, 25, 102100. <https://doi.org/10.1016/j.eti.2021.102100>
93. Su, G.; Xiong, J.; Li, Q.; Luo, S.; Zhang, Y.; Zhong, T.; ... & Xu, K. Gaseous formaldehyde adsorption by eco-friendly, porous bamboo carbon microfibers obtained by steam explosion, carbonization, and plasma activation. *Chemical Engineering Journal*, **2023**, 455, 140686. <https://www.sciencedirect.com/science/article/abs/pii/S1385894722061666>
94. Tahraoui, H.; Amrane, A.; Belhadj, A. E. & Zhang, J. Modeling the organic matter of water using the decision tree coupled with bootstrap aggregated and least-squares boosting. *Environmental Technology & Innovation*, **2022**, 27, 102419. <https://doi.org/10.1016/j.eti.2022.102419>
95. Tao, W. W.; Li, Q. T.; Zhou, T. Y. & Zhuang, D. D. The influence of ultrasonic assistance on microstructure and properties of AlCoCrFeNi high-entropy alloy prepared by laser cladding. *Journal of Materials Research and Technology*, **2024**, 29, 5161-5165. <https://doi.org/10.1016/j.jmrt.2024.03.015>
96. Tawfik, A. M. & Eltabey, R. M. Fractional kinetic strategy toward the adsorption of organic dyes: finding a way out of the dilemma relating to pseudo-first-and pseudo-second-order rate laws. *The Journal of Physical Chemistry*, **2024**, 128(6), 1063-1073. <https://pubs.acs.org/doi/abs/10.1021/acs.jpca.3c07615>
97. Thommes, M.; Kaneko, K.; Neimark, A. V.; Olivier, J. P.; Rodriguez-Reinoso, F.; Rouquerol, J. & Sing, K. S. Physisorption of gases, with special reference to the evaluation of surface area and pore size distribution (IUPAC Technical Report). *Pure and applied chemistry*, **2015**, 87(9-10), 1051-1069. <https://doi.org/10.1515/pac-2014-1117>
98. Tian, J.; Wang, Y. & Chen, Z. An improved single particle model for lithium-ion batteries based on main stress factor compensation. *Journal of Cleaner Production*, **2021**, 278, 123456. <https://doi.org/10.1016/j.jclepro.2020.123456>
99. Tileuberdi, Y., Ongarbayev, Y. K., Mansurov, Z. A., Kudaibergenov, K. K., & Doszhanov, Y. O. (2014). Ways of using rubber crumb from worn tires. *Applied Mechanics and Materials*, 446, 1512-1515. <https://www.scientific.net/AMM.446-447.1512>
100. Tunay, S.; Koklu, R. & Imamoglu, M. Highly Efficient and Environmentally Friendly Walnut Shell Carbon for the Removal of Ciprofloxacin, Diclofenac, and Sulfamethoxazole from Aqueous Solutions and Real Wastewater. *Processes*, **2024**, 12(12), 2766. <https://doi.org/10.3390/pr12122766>
101. Wang, H.; Zhang, Q.; Zhang, X.; Zhang, K.; Zhao, X.; Zhang, R. & Zhang, Z. NIR laser-activated polydopamine-coated Fe₃O₄ nanoplatfrom used as a recyclable precise photothermal insecticide. *Sustainable Materials and Technologies*, **2022**, 33, e00456. <https://doi.org/10.1016/j.susmat.2022.e00456>
102. Wang, T.; Zhang, D.; Fang, K.; Zhu, W.; Peng, Q. & Xie, Z. Enhanced nitrate removal by physical activation and Mg/Al layered double hydroxide modified biochar derived from wood waste: Adsorption characteristics and mechanisms. *Journal of Environmental Chemical Engineering*, **2021**, 9(4), 105184. <https://doi.org/10.1016/j.jece.2021.105184>
103. Wang, X.; Chai, X.; Huang, W.; Li, X.; Zhu, B.; Li, X. & Fu, L. Green synthesis of biomass-derived porous carbon with hierarchical pores and enhanced surface area for superior VOCs adsorption. *Materials Today Communications*, **2024**, 39, 108906. <https://doi.org/10.1016/j.mtcomm.2024.108906>
104. Wang, Z.; Wang, T.; Si, B.; Watson, J. & Zhang, Y. Accelerating anaerobic digestion for methane production: Potential role of direct interspecies electron transfer. *Renewable and Sustainable Energy Reviews*, **2021**, 145, 111069. <https://doi.org/10.1016/j.rser.2021.111069>
105. Wei, X.; Huang, S.; Yang, J.; Liu, P.; Li, X.; Xue, R.; ... & Wu, S. Adsorption of methylene blue on activated carbons prepared from penicillin mycelial residues via torrefaction and hydrothermal pretreatment. *Biomass Conversion and Biorefinery*, **2024**, 14(22), 28933-28945. <https://link.springer.com/article/10.1007/s13399-023-03998-0>

106. Xi, H.; Li, Q.; Yang, Y.; Zhang, J.; Guo, F.; Wang, X.; ... & Ruan, S. Highly effective removal of phosphate from complex water environment with porous Zr-bentonite alginate hydrogel beads: Facile synthesis and adsorption behavior study. *Applied Clay Science*, **2021**, 201, 105919 <https://doi.org/10.1016/j.clay.2020.105919>
107. Xu, M.; Zeng, Q.; Li, H.; Zhong, Y.; Tong, L.; Ruan, R. & Liu, H. Contribution of glycerol addition and algal-bacterial cooperation to nutrients recovery: a study on the mechanisms of microalgae-based wastewater remediation. *Journal of Chemical Technology & Biotechnology*, **2020**, 95(6), 1717-1728. <https://doi.org/10.3390/jcs6100311>
108. Yang, J.; Ma, X.; Xiong, Q.; Zhou, X.; Wu, H.; Yan, S. & Zhang, Z. Functional biochar fabricated from red mud and walnut shell for phosphorus wastewater treatment: Role of minerals. *Environmental Research*, **2023**, 232, 116348. <https://doi.org/10.1016/j.envres.2023.116348>
109. Yang, L.; Yungang, W.; Tao, L.; Li, Z.; Yanyuan, B. & Haoran, X. High-performance sorbents from ionic liquid activated walnut shell carbon: An investigation of adsorption and regeneration. *RSC advances*, **2023**, 13(33), 22744-22757. <https://pubs.rsc.org/en/content/articlehtml/2023/ra/d3ra03555g>
110. Zhanli, B. L. G. L.; Tang, W. & Chen, J. N-doped and activated porous biochar derived from cocoa shell for removing norfloxacin from aqueous solution: Performance assessment and mechanism insight. *Environmental Research*, **2022**, 214, 113951. <https://doi.org/10.1016/j.envres.2022.113951>
111. Zhan, L.; Zhang, X.; Zeng, Y.; Li, R.; Song, X. & Chen, B. Life cycle assessment of optimized cassava ethanol production process based on operating data from Guangxi factory in China. *Biomass Conversion and Biorefinery*, **2024**, 14(21), 26535-26552. <https://link.springer.com/article/10.1007/s13399-022-03442-9>
112. Zhang, G.; Lei, B.; Chen, S.; Xie, H. & Zhou, G. Activated carbon adsorbents with micro-mesoporous structure derived from waste biomass by stepwise activation for toluene removal from air. *Journal of Environmental Chemical Engineering*, **2021**, 9(4), 105387. <https://doi.org/10.1016/j.jece.2021.105387>
113. Zhang, H.; Gao, S.; Ji, Z.; Cui, J. & Pei, Y. Solidification/stabilization of organic matter and ammonium in high-salinity landfill leachate concentrate using one-part fly ash-based geopolymers. *Journal of Environmental Chemical Engineering*, **2023**, 11(2), 109379. <https://doi.org/10.1016/j.jece.2023.109379>
114. Zhang, H.; Zhang, Y.; Zhao, Y.; Liang, T.; Wei, W.; Zhang, W., ... & Tao, H. Magnetic biochar derived from dairy manure for peroxymonosulfate activation towards bisphenol A degradation: kinetics, electron transfer mechanism, and environmental toxicity. *Journal of Water Process Engineering*, **2022**, 50, 103314. <https://doi.org/10.1016/j.jwpe.2022.103314>
115. Zhang, L.; Yang, L.; Chen, J.; Yin, W.; Zhang, Y.; Zhou, X. ... & Zhao, J. Adsorption of Congo red and methylene blue onto nanopore-structured ashitaba waste and walnut shell-based activated carbons: Statistical thermodynamic investigations, pore size and site energy distribution studies. *Nanomaterials*, **2022**, 12(21), 3831. <https://www.mdpi.com/2079-4991/12/21/3831>
116. Zhang, Z.; Li, Y.; Ding, L.; Yu, J.; Zhou, Q.; Kong, Y. & Ma, J. Novel sodium bicarbonate activation of cassava ethanol sludge derived biochar for removing tetracycline from aqueous solution: Performance assessment and mechanism insight. *Bioresource Technology*, **2021**, 330, 124949. <https://doi.org/10.1016/j.biortech.2021.124949>
117. Zhao, H.; Yu, Q.; Li, M. & Sun, S. Preparation and water vapor adsorption of "green" walnut-shell activated carbon by CO₂ physical activation. *Adsorption Science & Technology*, **2020**, 38(1-2), 60-76. <https://journals.sagepub.com/doi/full/10.1177/0263617419900849>
118. Zhao, Y.; Cui, H.; Xu, J.; Shi, J.; Yan, R.; Yan, N. & Guo, H. Synthesis of biomimetic N-doped porous carbons from gelatin using salt template coupled with chemical activation strategy for CO₂ capture. *Chemical Engineering Journal*, **2025**, 505, 159241. <https://doi.org/10.1016/j.cej.2025.159241>
119. Zhou, X.; Li, X.; Guo, L.; Liu, X. & Liu, Y. 2, 4-Dichlorophenol removal from water by walnut shells-based biochar. *Desalination and Water Treatment*, **2022**, 252, 276-286. <https://doi.org/10.5004/dwt.2022.28261>
120. Zhu, G.; Jin, Y. & Ge, M. Simple and green method for preparing copper nanoparticles supported on carbonized cotton as a heterogeneous Fenton-like catalyst. *Colloids and Surfaces A: Physicochemical and Engineering Aspects*, **2022**, 647, 128978. <https://doi.org/10.1016/j.colsurfa.2022.128978>
121. Zou, W.; Zhang, M.; Zhang, X.; Zhang, D.; Li, C.; Zhong, L.; ... & Ngo, H. H. Optimized performance and mechanistic analysis of tetracycline hydrochloride removal using biochar-based alginate composite

magnetic beads for peroxymonosulfate activation. *Journal of Environmental Chemical Engineering*, **2025**, 115742. <https://doi.org/10.1016/j.jece.2025.115742>

Disclaimer/Publisher's Note: The statements, opinions and data contained in all publications are solely those of the individual author(s) and contributor(s) and not of MDPI and/or the editor(s). MDPI and/or the editor(s) disclaim responsibility for any injury to people or property resulting from any ideas, methods, instructions or products referred to in the content.